A cyclic nucleotide-gated channel is essential for polarized tip growth of pollen

Sabine Frietsch*, Yong-Fei Wang‡, Chris Sladek*, Lisbeth R. Poulsen§, Shawn M. Romanowsky*, Julian I. Schroeder‡, and Jeffrey F. Harper*¶

*Biochemistry Department MS200, University of Nevada, Reno, NV 89557; ‡Division of Biological Sciences, University of California at San Diego, La Jolla, CA 92093-0116; and §Centre for Membrane Pumps in Cells and Disease (PUMPKIN), Department of Plant Biology, Copenhagen University, DK-1871 Frederiksberg C, Denmark

Edited by Maarten J. Chrispeels, University of California at San Diego, La Jolla, CA, and approved July 9, 2007 (received for review February 26, 2007)

Ion signals are critical to regulating polarized growth in many cell types, including pollen in plants and neurons in animals. Genetic evidence presented here indicates that pollen tube growth requires cyclic nucleotide-gated channel (CNGC) 18. CNGCs are nonspecific cation channels found in plants and animals and have well established functions in excitatory signal transduction events in animals. In *Arabidopsis*, male sterility was observed for two *cngc18* null mutations. *CNGC18* is expressed primarily in pollen, as indicated from a promoter::*GUS* (*β-glucuronidase*) reporter analysis and expression profiling. The underlying cause of sterility was identified as a defect in pollen tube growth, resulting in tubes that were kinky, short, often thin, and unable to grow into the transmitting tract. Expression of a GFP-tagged CNGC18 in mutant pollen provided complementation and evidence for asymmetric localization of CNGC18 to the plasma membrane at the growing tip, starting at the time of pollen grain germination. Heterologous expression of CNGC18 in *Escherichia coli* resulted in a time- and concentration-dependent accumulation of more Ca^{2+}. Thus, CNGC18 provides a mechanism to directly transduce a cyclic nucleotide (cNMP) signal into an ion flux that can produce a localized signal capable of regulating the pollen tip-growth machinery. These results identify a CNGC that is essential to an organism's life cycle and raise the possibility that CNGCs have a widespread role in regulating cell-growth dynamics in both plant and animals.

calcium | male sterile | *Arabidopsis* | CaM

In eukaryotes, there are many examples of cells that undergo polarized growth, such as neurons in animals and pollen tubes in flowering plants (1, 2). Pollen provide a powerful model system to study fundamental questions about polarized tip growth (3), including the underlying role of ion fluxes in signal transduction. Cation fluxes across the pollen tube plasma membrane have been well documented for H^+, K^+, and Ca^{2+} (3–7). However, the identification of specific ion transporters and their biological functions remains a challenge, considering that as many as 1,046 membrane transporters are expressed during pollen development (8, 9).

Fertilization in flowering plants requires that pollen tubes grow long distances in search of fertile ovules (3). This journey is not a process of random growth, but rather involves a directional mechanism in which the pollen tube tip responds to guidance signals. Ca^{2+} signals have been shown to regulate many polarized growth systems, including neurons, fungal hyphae, fern/moss protonema, rhizoids in a marine brown algae, as well as root hairs and pollen in plants (1, 2). In some systems, such as pollen tube tip growth, there is evidence that cytosolic cyclic nucleotide (cNMP) signals can trigger a growth-altering Ca^{2+} signal (10). One target of cNMP signals in both plants and animals is the family of nonspecific cyclic nucleotide-gated ion channels (CNGCs), which provides a mechanism to directly transduce a cNMP signal into a cation flux across the plasma membrane.

In mammals, there are only six CNGC isoforms reported (11). Nevertheless, there are numerous examples of animal *cngc* mutations that cause blindness, taste defects, and neuronal disorders (11). In contrast, plants appear to have many more CNGCs, with only a few mutant phenotypes so far reported. In *Arabidopsis*, there are 20 CNGCs, with at least 1 CNGC isoform expressed in each of the major tissues (12). Molecular genetic studies in plants have established that CNGCs can function in modifying plant development as well as a plant's response to pathogens and abiotic stresses, such as heavy metals and high levels of calcium or sodium (12–18). Until now, only nonlethal phenotypes have been associated with CNGC mutations or "knock-down" lines in either plants or animals (11, 12, 15).

Here, we provide genetic evidence for a CNGC that is essential to the life cycle of a flowering plant. Two loss-of-function mutations in *CNGC18* were found to cause male sterility in *Arabidopsis thaliana*, with the underlying defect being a disruption in pollen tube tip growth. An asymmetric localization of GFP-CNGC18 at the plasma membrane of the growing tip supports a direct role of CNGC18 in regulating the tip-growth machinery. Heterologous expression of CNGC18 in *Escherichia coli* results in the accumulation of more Ca^{2+}. Together, these findings provide strong evidence for a mechanism of polarized growth in pollen tubes involving a cation channel that can directly transduce a cyclic nucleotide signal into a growth-altering ion flux. These findings also raise the consideration that CNGCs may have a more widespread role in regulating cell growth and morphology in both plants and animals.

Results

Two independent *cngc18* T-DNA [portion of the Ti (tumor-inducing) plasmid that is transferred to plant cells] gene disruptions were identified from two different *Arabidopsis* T-DNA mutant collections, *cngc18-1* (19) and *cngc18-2* (20). The insertions were found to disrupt coding sequence in exons 5 and 1 of *CNGC18* (*At5g14870*), respectively (Fig. 1), as shown by DNA sequencing of the region adjacent to the T-DNA left border [supporting information (SI) *Appendix*, section S1]. Both knockouts were backcrossed twice and confirmed to have single insertions displaying 100% cosegregation between the T-DNA resistance marker and the *CNGC18*-T-DNA border ($n = 186$ and

Author contributions: S.F. and J.F.H. designed research; S.F., Y.-F.W., C.S., and L.R.P. performed research; S.M.R., J.I.S., and J.F.H. contributed new reagents/analytic tools; S.F. and J.F.H. analyzed data; and S.F. and J.F.H. wrote the paper.

The authors declare no conflict of interest.

This article is a PNAS Direct Submission.

Abbreviations: CNGC, cyclic nucleotide-gated channel; T-DNA, portion of the Ti (tumor-inducing) plasmid that is transferred to plant cells; cNMP, cyclic nucleotides; ACA9, Auto-inhibited-Ca^{2+}-ATPase 9; SPIK, shaker pollen inward K^+ channel; GUS, β-glucuronidase; ss no., seed stock number.

¶To whom correspondence should be addressed at: Biochemistry Department MS200, University of Nevada, Reno, 1664 North Virginia Street, Reno, NV 89557. E-mail: jfharper@unr.edu.

This article contains supporting information online at www.pnas.org/cgi/content/full/0701781104/DC1.

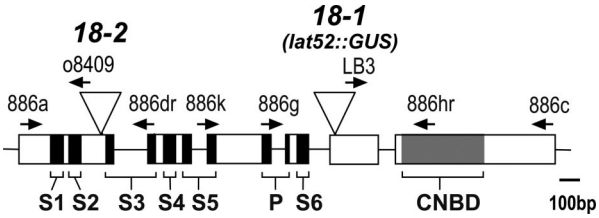

Fig. 1. Diagram showing *CNGC18* T-DNA disruptions. The diagram illustrates the genomic structure of *CNGC18* (*At5g14870*), including the T-DNA insertion sites (triangles) of *cngc18-1* and *18-2*, 1,555 and 435 bp downstream of the start codon, respectively. The T-DNA of *cngc18-1* encodes a pollen-expressed *lat52*-promoter::*GUS*. Rectangles, exons; -, introns; black filled parts of squares, transmembrane (S1–S6) and pore (P) domains; gray shading, cyclic nucleotide binding domain (CNBD); →, position of the primers. (Scale bar, 100 bp.)

$n = 65$, respectively). When plant lines heterozygous for *cngc18-1* and *18-2* (−/+) were allowed to self-fertilize, we observed a non-Mendelian 1:1 segregation ratio (+/+ to −/+) as determined by herbicide resistance and PCR analysis of the T-DNA insertion site (Table 1, Group A). The observed segregation distortion suggests a potential lethal effect in either the male or female gametophyte. Evidence confirming a defect in the male gametophyte was obtained by reciprocal crosses between *cngc18-1* (−/+) and WT plants, as well as by outcrossing to male sterility 1 plants (*ms1-1*) (21) (Table 1, Group B). Although we observed the expected 1:1 transmission of the *cngc18* mutant allele through the female gametophyte ($n = 20$), we never observed transmission of the mutant allele through the pollen ($n = 37$ and $n = 120$, respectively). These crosses show that *cngc18-1* and *18-2* result in sterile pollen, with no indication of a defect in the female gametophyte.

Complementation. To provide confirmation that *cngc18-1* male sterility resulted from a loss-of-function mutation, we tested for complementation by transforming *cngc18-1* (−/+) plants with a 6.88-kb fragment of genomic DNA (*gCNGC18*) harboring *CNGC18* (*SI Appendix*, Fig. S9*A*). Within this genomic fragment, *CNGC18* is predicted to be the only complete gene (www.tigr.org, accessed on August 1, 2005). Complementation by *gCNGC18* was verified by a segregation analysis. In six of six transgenic lines analyzed, the *cngc18-1* allele was found to segregate in a normal Mendelian fashion (Table 1, Group C). A PCR diagnostic analysis of selected plants confirmed that complementation resulted in the segregation of plants homozygous for the *cngc18-1* T-DNA disruption (data not shown). As described later, complementation was also observed by using a GFP-tagged CNGC18 expressed under the control of a pollen-specific promoter (Table 1, Group C).

***CNGC18* Is Expressed in Pollen.** To evaluate the developmental and tissue-specific expression pattern of *CNGC18*, a 3.35-kb upstream region of *CNGC18* was fused to the reporter gene encoding *β-glucuronidase* (*GUS*) (*SI Appendix*, Fig. S9*B*) and transformed into *Arabidopsis* plants. Histochemical staining of tissues from transgenic plants demonstrated GUS activity in the pollen grains, but not in leaves, roots, or root hairs of young seedlings (*SI Appendix*, Fig. S2 *A–H*). The observed expression pattern was confirmed by an analysis of >2,489 publicly available microarray datasets (*SI Appendix*, Fig. S2*I*) that were made searchable at the Genevestigator database (22). Together, our results indicate that *CNGC18* is preferentially or specifically expressed in pollen.

CNGC18 Is Essential for Directional Pollen Tube Growth *in Vitro*. Initial analysis of pollen viability and seed set indicated that *cngc18* pollen is properly developed and does not compete with WT pollen or block fertilization (*SI Appendix*, Fig. S3 *A–C*), as seen in some male gametophyte defective mutants [e.g., autoinhibited-Ca^{2+}-ATPase 9 (ACA9) (23)]. *In vitro* assays established equal germination rates for control and *cngc18* pollen (*SI Appendix*, Section S4). However, *cngc18* pollen tubes showed a severe growth defect. In comparison to tetrads from *qrt* controls, which produced up to four normally developed pollen tubes (Fig. 2*A*), *cngc18-1* tetrads developed "kinky," short, and often thin pollen tubes with high frequency (Fig. 2 *B–D*). The kinky pollen tubes only grew a short distance with nondirectional growth, often prematurely terminating with a bursting event. Similar morphologies were observed in *cngc18-2* pollen tubes (data not shown).

To carefully evaluate the pollen-tube growth defect, a total of 735 WT and 712 *cngc18-1* tetrads were individually scored for "healthy"/normal or aberrant pollen tube morphologies. The *qrt* background of *cngc18-1* plants allowed us to simultaneously examine all four meiotic products, consisting of two WT and two mutant pollen grains. Fig. 2*E* shows the frequency of mutant and *qrt* control tetrads that developed only healthy pollen tubes (i.e., no aberrant

Table 1. Segregation analysis identifying non-Mendelian transmission of the T- DNA in *cngc18* mutants

Group	Parent, Female × Male	Segregation of resistance gene			
		Total	Expected	Observed	Transmission, %
A	*cngc18-1*, selfed	802	602	426*,†,‡	53*,†,‡
	cngc18-2, selfed	300	225	143*,†,‡	48*,†,‡
B	WT × *cngc18-1*	37	19	0	0
	cngc18-1 × WT	20	10	10	50
	ms1-1 × *cngc18-1*	120	60	0	0
C	*gCNGC18*, selfed	437	328	349§	79.9§
	GFP-CNGC18, selfed	873	655	626§	71.7§

Group A: self-fertilized *cngc18* mutants (*cngc18*, selfed). Group B: reciprocal crosses with WT and *male sterility1* (*ms1-1*) plants (21) obtained from the *Arabidopsis* Biological Resource Center (ABRC; stock CS75). Group C: self-fertilized F_2 progeny of *cngc18-1* plants complemented with a genomic construct (*gCNGC18*, selfed) or the GFP-tagged cDNA of *CNGC18* (*GFP-CNGC18*, selfed). The observed resistance (observed) was compared to an expected Mendelian segregation of 75% resistance (expected). Statistical significance was determined by Pearson's χ^2 test. The transmission of the T-DNA to the next progeny was calculated as (total/100) × observed resistance.

*Significantly different from Mendelian segregation ratio 3:1 (χ^2, $P < 0.01$).

†Significantly different from segregation ratio 2:1 (χ^2, $P < 0.01$).

‡Not significantly different from segregation ratio 1:1 (χ^2, $P > 0.01$).

§Not significantly different from Mendelian segregation ratio 3:1 (χ^2, $P > 0.01$).

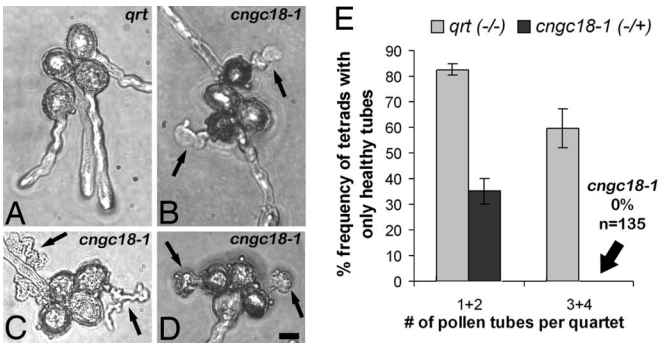

Fig. 2. *In vitro* germination assays reveal aberrant morphologies of *cngc18* pollen tubes. (*A*) A germinated tetrad from the *qrt* parental control lines showing four normal/healthy pollen tubes. (*B–D*) Representative tetrads from *cngc18-1* (ss no. 130) showing segregation of healthy and aberrant pollen tubes. (Scale bar in *A–D*, 10 μm.) (*E*) Frequency of tetrads in which all of the germinated pollen grains produced healthy pollen tubes. Pollen tubes were considered aberrant if they had kinky morphologies or failed to grow >50 μm. The graph shows the frequency of tetrads consisting of one or two tubes (1 + 2) with normal/healthy morphology (*qrt*: $n = 520$; *cngc18-1*: $n = 577$) versus three or four pollen tubes (3 + 4) (*qrt*: $n = 215$; *cngc18-1*: $n = 135$). The analysis was done in three independent experiments with similar germination frequencies in each analysis. No *cngc18-1* tetrads were observed with more than two healthy tubes, as indicated by the position of an arrow.

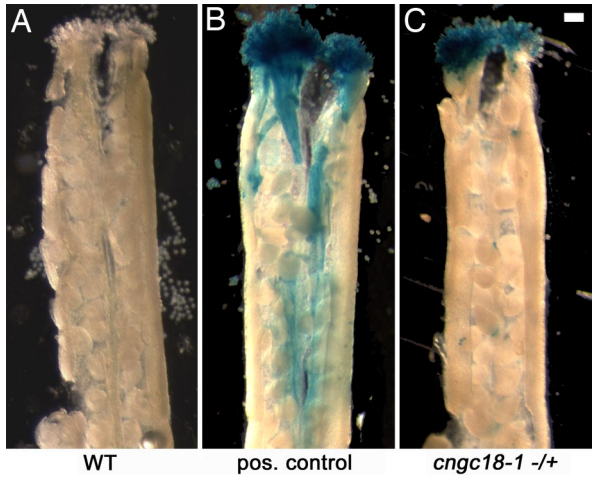

Fig. 3. Histochemical staining for a *cngc18*-linked GUS-reporter demonstrates that mutant pollen never enter the transmitting tract. Representative example of GUS-stained pistils fertilized with pollen from WT (*A*), positive controls (pos. control) (*B*), and *cngc18-1* (−/+) plants (ss no. 578) (*C*). Pistils were dissected and stained for GUS activity as described in ref. 27. Plant lines used for *cngc18-1* and the positive control harbored a pollen-specific *lat-52*::*GUS* reporter within their respective T-DNA insertions (19). (Scale bar, 0.1 mm.)

morphologies). In cases where tetrads only germinated one or two pollen tubes (1 + 2), the mutant tetrads showed a dramatic reduction (≈2-fold) in the frequency of tetrads with only healthy pollen tubes. This finding is consistent with the expectation that 50% of these tubes are segregating as mutant pollen. In the 135 cases in which the mutant tetrads produced more than two visible tubes (3 + 4), we never observed a single example in which more than two of the tubes were healthy. Thus, these results demonstrate that the *cngc18*-null mutation results in a pollen tube growth defect when grown *in vitro*.

***cngc18* Pollen Tubes Failed to Grow into the Transmitting Tract.** The *in vitro* pollen-tube growth defect of *cngc18* was corroborated *in vivo* by histochemical staining of *cngc18-1* pollen growing in pistils of WT plants. The T-DNA of *cngc18-1* harbors a pollen-expressed *lat52*-promoter::*GUS* reporter (Fig. 1) (19). Because this reporter construct is linked to the *cngc18-1* mutation, it allowed us to use GUS staining to differentiate between mutant and WT pollen tubes produced from a *cngc18-1* (−/+) plant.

Pollen from a *cngc18-1* flower was used to manually pollinate WT pistils. After 24 h, fertilized pistils were stained for GUS activity. For a positive control, a parallel pollination was performed with WT and pollen that harbored a *lat52*-promoter::*GUS* construct inserted in a phenotypically silent location. For all 20 positive control pollinations, we always observed blue-stained pollen tubes that grew to the bottom of the transmitting tract (Fig. 3*B*). In contrast, none of the 10 pistils pollinated with *cngc18-1* pollen showed any evidence for GUS-stained pollen tubes entering the transmitting tract (Fig. 3*C*), even after increased incubation times in the GUS-staining solution. Instead, GUS staining was restricted to the stigma, or wherever a pollen grain had landed during the experiment. These results are consistent with the *in vitro* assays that indicate a directional growth defect and demonstrate that this defect prevents *cngc18-1* pollen from growing into the transmitting tract.

CNGC18 Localizes to the Plasma Membrane at the Pollen Tube Tip. The potential subcellular localization of CNGC18 was investigated by expressing a transgene encoding an N-terminal GFP-tagged CNGC18 (GFP-CNGC18) under the control of a pollen-specific promoter (*SI Appendix*, Fig. S9*C*). This construct was shown to provide complementation of *cngc18-1* (−/+) in 41 of 42 independent transgenic lines (Table 1).

The subcellular localization of GFP-CNGC18 was evaluated with confocal fluorescence microscopy (Fig. 4). For comparisons, we conducted parallel analyses on pollen tubes expressing a GFP-only

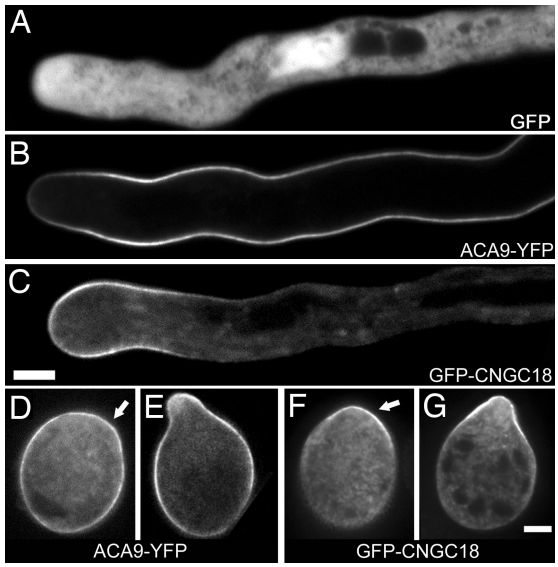

Fig. 4. Confocal fluorescence micrographs showing asymmetric localization of GFP-CNGC18 in pollen grains and tubes. Pollen were germinated *in vitro* and analyzed in parallel: WT plants expressing GFP (ss no. 464) (*A*), *aca9-1* mutants complemented with ACA9-YFP (ss no. 471 and 472) (*B*, *D*, and *E*) (23), and *cngc18-1* plants complemented with GFP-CNGC18 (*C*, *F*, and *G*). Three developmental stages were analyzed: fully grown pollen tubes (*A–C*), pollen grains with initial germination bulge (*D* and *F*), and pollen grains with emerging tip (*E* and *G*). The images shown all represent GFP signals and not background autofluorescence, as determined by comparisons with WT pollen imaged side-by-side with the same exposures. Due to different fluorescence intensities, exposure times in the images shown are 0.5 sec (*A*), 3 sec (*B*), and 6 sec (*C–G*). (Scale bar, 5 μm.)

control as a marker for the cytosol (Fig. 4*A*) and ACA9-YFP as a marker for the plasma membrane (Fig. 4*B*) (23). In comparison, GFP-CNGC18 showed distinct pattern of localization, with the most intense signal focused at the cell perimeter of the growing pollen tube tip, consistent with a tip-focused plasma membrane location (Fig. 4*C*). In addition, we observed some association of GFP-CNGC18 with small vesicles that were engaged in cytoplasmic streaming (see *SI Appendix*, Movie S5).

We also imaged GFP-CNGC18 during pollen grain germination and tip emergence. Early-staged hydrated pollen grains displayed a diffuse GFP-CNGC18 expression that could not be attributed to the plasma membrane or another specific compartment (*SI Appendix*, Fig. S6 *B–F*). However, at latter stages, a polarized localization developed at the first visible bulge, presumed to be the point of pollen tube emergence (Fig. 4 *F* and *G* and *SI Appendix*, Fig. S6 *G–V*).

Expression of CNGC18 in *E. coli* Results in Increased Ca^{2+} Accumulation. To evaluate whether CNGC18 activity could alter Ca^{2+} influx across the plasma membrane, we measured the accumulation of 14 different ions in *E. coli* cells expressing CNGC18 compared with a vector control. The relative levels of Cu, Ca, Fe, K, Li, Mg, Mn, Na, Ni, P, S, Zn, as well as Gd and Rb (if applicable), were determined by using inductively coupled plasma atomic-emission spectroscopy (ICP-AES) (*SI Appendix*, Fig. S7). In multiple independent analyses ($n = 27$) using several different media compositions, CNGC18 expression always resulted in a large relative increase in Ca^{2+} accumulation. In the uptake experiments shown in Fig. 5*A*, relative levels were 1.7-fold higher in CNGC18-expressing cells compared with control cells, after incubation for 1 h in media containing 10 mM each of Ca^{2+}, Rb^{+}, and Na^{+}. This Ca^{2+} accumulation was specifically inhibited by 0.1 mM Gd^{3+}, a broad specificity Ca^{2+} channel blocker (Fig. 5*B*). Ca^{2+} accumulation was time-dependent (Fig. 5*C*) and concentration-dependent (Fig. 5*D*). Fourteen dose–response experiments at earlier (10–15 min) and later time points (45–60 min) showed that CNGC18 increased the Ca^{2+} accumulation in cells. The differences were larger when examined at later time points (Fig. 5*D*). These results are consistent with an increased expression of Ca^{2+}-permeable channels in *E. coli*.

CNGC18 expression also resulted in an apparent reduction of K^{+} and Mg^{2+} under the conditions used in Fig. 5*A*. In the experiment shown, Rb^{+} was used as a K^{+} analog, providing supporting evidence that CNGC18 can also change K^{+} homeostasis in *E. coli*. In contrast, the accumulation of Na^{+} did not show significant changes during these experiments, presumably because the 10 mM external sodium was near equilibrium with the internal Na^{+} concentration. Although this is consistent with the expectation from other CNGC research showing that K^{+} and other cations are permeable (11, 12), these experiments were designed to only test for Ca^{2+} permeability. Additional dose-dependent flux measurements would be necessary to confirm a K^{+} and Na^{+} conductance of CNGC18.

Discussion

Genetic evidence presented here identifies 1 of the 20 CNGCs encoded in *A. thaliana* as essential for the plant's life cycle. Null mutations of *CNGC18* resulted in defective pollen tubes that were unable to undergo directional growth (Fig. 2 *B–D*) and reach the ovule for fertilization (Fig. 3). The *cngc18* pollen defects are consistent with promoter-*GUS* reporter analyses and expression profiling studies that indicate that CNGC18 is expressed primarily in pollen (*SI Appendix*, Fig. S2). Although five additional CNGC isoforms are expressed in *Arabidopsis* pollen, their functions in fertilization are not yet clear.

Although there are numerous examples of *cngc* mutations in animals, all phenotypes are currently linked to nonlethal defects such as blindness, taste defects, and neuronal disorders (11, 24, 25). Although CNGCs are expected to have a functional role in mammalian reproduction, the first gene knockout in mice for one of the three sperm CNGCs (subunit A3) did not result in a fertility defect (11, 26).

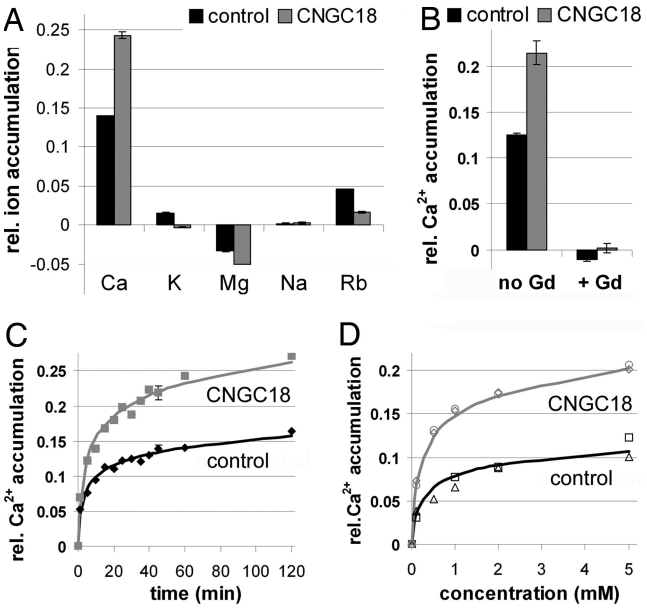

Fig. 5. CNGC18 expression results in increased Ca^{2+} accumulation in *E. coli*. (*A* and *B*). Representative examples of Ca^{2+} accumulation (average of $n = 3$) during 1 h of incubation in a 2% lactose solution containing 10 mM each of $CaCl_2$, NaCl, and RbCl (*A*) and additional 0.1 mM $GdCl_3$ (*B*). (*C*) Representative Ca^{2+} accumulation profiles >120 min in same medium as used in *A* ($n = 3$ for 0, 45, 60, and 120 min). (*D*) Relative Ca^{2+} accumulation during 40-min incubation in 2% lactose solution containing 0.1–5 mM $CaCl_2$, NaCl, and RbCl (equimolar). All ion accumulation profiles were determined by using inductively coupled plasma atomic-emission spectroscopy and were normalized to equal levels of P as an internal standard. Although selected experiments were also normalized to fresh weight (for example, see *SI Appendix*, Fig. S7), the use of P as an internal standard was operationally found to be a more consistent normalization factor. A similar strategy was also found to be more reliable in comparing small amounts of plant tissue (48). The relative Ca^{2+} accumulation ratio shown can be converted to an estimated ppm/g fresh weight by multiplying with a conversion factor of 200. This conversion factor was experimentally determined from multiple inductively coupled plasma analyses conducted on larger samples, which could be more accurately weighed.

***cngc18* Defines a Unique Pollen Tube Growth Phenotype.** More than 13,900 genes are expected to be involved in controlling the many aspects of pollen development (9). Although many pollen development mutations have been isolated, relatively few have been characterized that show a defect in pollen tube growth.

For example, in a mutant screen through >10,000 T-DNA mutant plants, 30 mutations called hapless (hap) were identified that disrupted some aspect of the male gametophyte (27). Among these, <50% (12) of the mutants were found to produce pollen that failed to grow into the transmitting tract. However, within this category of mutants, there can be multiple causes, including a failure of pollen to germinate or undergo directional growth. In the case of *cngc18*, we provide evidence from *in vitro* growth assays that the underlying defect was not related to germination but rather to a growth defect producing pollen tubes that were short, kinky, often thin, and frequently bursting after a short period of growth (Fig. 2 *B–D*).

Similar kinky morphologies have also been observed for pollen tubes from three other mutants; two from T-DNA disruptions in genes encoding cell wall-modifying proteins *kinky pollen* (*kip*) and *vanguard1* mutants, as well as *crinkle* (*crk*), an ethyl methanesulfonate (EMS) mutant selected for its root-hair defect that

disrupts nodulation in *Lotus japonicus* (28). However, none of these mutations result in complete male sterility (like *cngc18*) and none have so far been implicated in the signal transduction events that coordinate tip growth.

At present, genetic analysis in search of pollen phenotypes has been presented for two other cation channels, tandem-pore K^+ channel and shaker pollen inward K^+ channel (SPIK; AKT5/6), which are annotated as K^+-selective channels. A loss-of-function mutation for tandem-pore K^+ channel failed to show any defect in pollen tube growth and fertilization (29), and a T-DNA insertion disrupting the C-terminal end of SPIK (AKT5/6) resulted in a weak segregation distortion (31% WT progeny versus the expected 25%) (30). Although half of the *spik* pollen tubes appear to grow long and straight, some tubes displayed a short, bulbous, growth arrested phenotype, with some similarities to *cngc18*. However, unlike *spik*, *cngc18* pollen never developed any healthy elongated tubes or showed evidence of growing into the transmitting tract. These differences in pollen tube growth and the inability to recover a homozygous CNGC18 mutant plant, indicates that CNGC18 has unique and essential functions distinct from K^+ channels SPIK and tandem-pore K^+ channel.

Asymmetric Subcellular Localization of CNGC18. Confocal microscopy of a GFP-tagged CNGC18 in pollen revealed a polarized localization at the growing pollen tip (Fig. 4 *C*, *F*, and *G*), consistent with a plasma membrane localization. This asymmetric pattern was very distinct from a more uniform plasma membrane distribution observed for a control YFP-tagged Ca^{2+} pump, ACA9 (Fig. 4 *B*, *D*, and *E*) (23). This polarized distribution of GFP-CNGC18 was also observed at the emerging pollen tip in germinating pollen grains.

A caveat to using a GFP tag for subcellular localization is that targeting artifacts may arise from either over-expression or the tag itself. Although we cannot completely rule out such artifacts in our study, it is important to note that the localization pattern presented in Fig. 4 was evident even in transgenic plant lines for which the level of GFP fluorescence was at its lower limits of detection. It is also important to note that the *GFP-CNGC18* construct provided complementation in 41 of 42 independent transgenic lines. Thus, we conclude that at least some of the observed GFP-tagged CNGC18 were targeted to a functionally correct location.

Our working hypothesis is that the plasma membrane represents the primary functional location of CNGC18, which is consistent with observations supporting a plasma membrane location for four other plant CNGCs expressed in vegetative cells (16, 31, 32). Nevertheless, detectable levels of fluorescence were also observed associated with vesicles (*SI Appendix*, Movie S5). It is possible that the accumulation of GFP-CNGC18 in nonplasma membrane locations is an artifact of overexpression, but it is also possible that such vesicles normally harbor a small amount of CNGC18 and function in (*i*) the trafficking of proteins into and out of the plasma membrane to create a tip-localized distribution of CNGC18 or as (*ii*) an internal source of Ca^{2+}.

The tip-focused localization of GFP-CNGC18 raises the potential that it may contribute to the regulation of the tip-focused cytosolic Ca^{2+} gradient (5). However, the localization of GFP-CNGC18 appears to be strongest at a region just behind the tip apex, which suggests that it is not the primary channel responsible for the major tip apex-centered Ca^{2+} influx that has been reported from electrophysiological studies (5, 6). Nevertheless, the more lateral positioning of GFP-CNGC18 to the sides of the tip is well suited for a potential key role in sensing and responding to directional cues, much like separation of two eyes or two ears provides the basis for depth perception or directional sensing.

Regardless of the specific functions of CNGC18, it is likely that several different types of cation channels will be involved in regulating pollen tube growth, including a reported stretch activated Ca^{2+} channel, K^+ channels (e.g., SPIK), glutamate receptors, and other pollen-expressed CNGCs (6, 9, 30). Whether any of these other cation channels display an asymmetric localization similar to GFP-CNGC18 has not yet been established.

A Calcium-Signaling CNGC Paradigm. Research on animal and plant CNGCs has provided a strong precedent that conventional CNGCs function as nonspecific cation channels regulated by cNMP and Ca^{2+}/calmodulin (11, 12). In animals, evidence indicates that the physiological functions of most CNGCs are dependent on their ability to trigger a change in the membrane potential and/or directly carry an inward Ca^{2+} current (11). However, a phylogenetically distinct CNGC from sea urchin, with a GYGD pore signature, has been shown to be K^+-selective (33, 34). For the few CNGCs characterized from plants, studies confirm them as nonspecific cation channels that can be activated by cAMP and cGMP and blocked by Ca^{2+}/calmodulin (12, 14, 18, 35, 36).

To test whether CNGC18 could function as a Ca^{2+}-permeable channel, we expressed a *CNGC18* construct in *E. coli* and evaluated cells for changes in ion uptake. We choose to pursue an *E. coli* expression system because heterologous expression of CNGCs in eukaryotic cells such as yeast or oocytes has been problematic (12, 37), possibly because of the presence of endogenous calmodulin that can bind and deactivate a CNGC (37). Recent studies have provided a precedent for using an *E. coli* expression system to functionally analyze eukaryotic cation transporters (14, 37). The *E. coli* ion accumulation experiments presented here provide evidence that CNGC18 is permeable to Ca^{2+} (Fig. 5). Although endogenous Ca^{2+} uptake mechanisms exist in *E. coli*, expression of CNGC18 increased Ca^{2+} accumulation in a dose- and time-dependent manner. These findings are consistent with the expression of CNGC18 adding more calcium-permeable channels to the *E. coli* membrane and increasing the net influx of calcium into the cell. Although further studies are needed to confirm ion conductance properties of CNGCs in plant cells, these transport studies support a working model in which CNGC18 could mediate Ca^{2+} transport across the plant plasma membrane (*SI Appendix*, Fig. S8).

Although our results cannot rule out that CNGC18-mediated ion fluxes contribute to the nutritional/osmotic ion balance of the pollen, we favor a model in which the functional role of CNGC18 is primarily for signal transduction, as expected from the animal paradigm. The primary evidence supporting this perspective is the unusual tip-focused localization observed for GFP-CNGC18. This pattern is distinct from the more uniformly distributed localization observed for a "house keeping" transporter, such as calcium pump ACA9 (23) or the pattern expected for a transporter functioning to scavenge nutrients from the environment.

A Model for CNGC18 in Polarized Tip Growth. Once pollen grains have germinated and initiated tip growth, their continued directional growth is a dynamic process that is sensitive to tropism signals that ultimately guide the pollen tube to the ovule for fertilization. An emerging model of pollen tube tip growth includes a key step in which tropism cues elicit a localized increase in a cNMP (5, 38) that subsequently triggers a local growth-altering increase in cytosolic Ca^{2+} (10, 39). The identification here of CNGC18 at the pollen tip provides a mechanism to directly transduce a cNMP signal into localized growth-altering Ca^{2+} signals (*SI Appendix*, Fig. S8). On the basis of the Ca^{2+} permeability of plant and animal CNGCs, we propose that CNGC18 could either directly induce a localized Ca^{2+} influx or indirectly open other Ca^{2+} channels through a cation flux-dependent change in the membrane potential (*SI Appendix*, Fig. S8), as observed for an unusual CNGC involved in chemotaxis of sea urchin sperm (33).

Pollen tube growth and guidance has frequently been compared with directional growth of neurons during animal development (40, 41). In support of this analogy, CNGC mutations and cell biological evidence support a role of CNGCs in neuronal tip growth (11, 42, 43). However, not all tip-growing cells rely on CNGCs for regulating directional growth. For example, fungal systems without obvious

CNGC orthologs still engage in directional tip growth, perhaps by using alternative Ca^{2+} channels, such as CCH1 (44). Nevertheless, the *cngc18* phenotype presented here establishes a paradigm for considering a more widespread role of CNGCs in the control of polarized growth processes in both plants and animals, such as tip growth in root hairs, the development of leaf trichomes, the elongated growth expansion of cells (such as found on the root epidermis), or the plethora of cell morphologies observed in animal systems.

Materials and Methods

Plant Lines and Growth Conditions. All *cngc18* mutants were in the Columbia ecotype of *A. thaliana*. The *cngc18-1* mutant [Sail 191_H04, seed stock number (ss no.) 130] (19) harbors a resistance marker for glufosinate ("basta"), whereas *cngc18-2* (Gabi 052_H11, ss no. 599) encodes a sulfadiazine resistance marker (20). Both *cngc18* mutant lines were backcrossed to WT two times to produce heterozygous seed stocks for *cngc18-1* (ss no. 578; no *qrt* phenotype) and *cngc18-2* (ss no. 760).

Seeds were germinated and grown on 0.5× Murashige and Skoog (MS) plates containing 1% agar and the following antibiotics as appropriate: glufosinate (10 μg/ml), sulfadiazine (11.25 μg/ml), and hygromycin (25 μg/ml). After 10–14 days, resistant plants were scored and transferred to soil. All plants were grown at 22°C, 70% humidity with a 16-h-light/8-h-dark photoperiod regime at ≈70 μmol m^{-2} s^{-1}.

Plasmid Constructs and Plant Transformation. Plants were transformed with *Agrobacterium* (GV3101) containing the helper plasmid pSoup, by using the floral dip method (45, 46). All plant constructs were cloned in a modified pGreen II transformation vector (46) providing kanamycin resistance in bacteria (50 μg/ml) and hygromycin resistance in plants. All PCR-derived constructs were verified by DNA sequencing. Complete construct sequences are provided in the supplement (*SI Appendix*, Figs. S11 and S12).

Pollen Tube Germination. Pollen were incubated for 30 min to 6 h on germination media, according to Fan *et al*. containing low-gelling-temperature agarose (A-6560; Sigma–Aldrich, St. Louis, MO) (47). The pistil and stamen of the flower were placed in proximity to the pollen on the germination media.

Fluorescent Microscopy. Fluorescence imaging of GFP and YFP proteins expressed in pollen was performed with spinning-disk confocal microscopy by using a QLC100 confocal scanning unit (Solamere Technology Group, Salt Lake City, UT) attached to a Nikon Eclipse TE 2000-U bright field microscope (Tokyo, Japan) and an argon laser with excitation wavelength at 488 nm (500 M Select; Laserphysics, West Jordan, UT). For filtering the emission wavelength, emitter HQ525/50 at 500–550 nm was used (Chroma Technology, Rockingham, VT). Images were captured with a CCD camera (CoolSnap HQ; Photometrics, Tucson, AZ) with MetaMorph software (Universal Imaging, Downingtown, PA).

Ion Accumulation Assay in *E. Coli*. *E. coli* cells (T7 Express Competent *E. coli*, C2566; New England Biolabs, Ipswich, MA) were transformed with a modified pQE expression plasmid (Qiagen, Hilden, Germany) containing a *TAP-GFP* (ps no. 616) or *TAP-GFP-CNGC18* (ps no. 1391) fusion construct under the control of an IPTG-inducible *T5*-promoter (*SI Appendix*, Figs. S10 and S12). Cells were grown in modified 2× YT media without NaCl (*SI Appendix*, Fig. S7). A culture with an optical density of 0.6 (OD_{600}) was induced with 0.1 mM isopropyl β-D-thiogalactoside (IPTG) for 2 h and expression of the respective construct was confirmed by visualizing GFP fluorescence. The cultures were washed and resuspended in 2% lactose (OD_{600} 1.1–1.3). For all experiments, three 2-ml replicates were aliquoted and washed after a brief preincubation. Afterward $CaCl_2$, RbCl, and NaCl were added at an equal final concentration of 0.1–10 mM. The *E. coli* cells were pelleted, washed twice with 2% lactose solution, and digested overnight in 1 ml of concentrated HNO_3. The ion content of a 1:5 diluted sample was determined by an inductively coupled plasma atomic emission spectroscopy (Varian, Palo Alto, CA).

We thank Ryan Davis, Greta Granstedt, Kathy Truong, and Citlali Villalobos for technical assistance; Stefan Binder, Josef Kuhn, Aurelien Boisson-Dernier, and Amy Curran for scientific advice and help with the manuscript. This work was supported by Boehringer Ingelheim Fonds predoctoral fellowship and grants (to S.F.), Centre for Membrane Pumps in Cells and Disease (PUMPKIN) (L.R.P.), the Department of Energy Grants DE-FG03-94ER20152 and DE-FC52-05NA26972 (to J.F.H.), National Institute of Health Grants R01GM070813 (to J.F.H.) and R01GM060396 (to J.I.S.), and National Science Foundation Awards DBI 0077378 and IBN-0419695 (to J.F.H. and J.I.S.).

1. Mattson MP (1999) *J Neurosci Res* 57:577–589.
2. Hepler PK, Vidali L, Cheung AY (2001) *Annu Rev Cell Dev Biol* 17:159–187.
3. Franklin-Tong VE (1999) *Plant Cell* 11:727–738.
4. Griessner M, Obermeyer G (2003) *J Membr Biol* 193:99–108.
5. Holdaway-Clarke TL, Hepler PK (2003) *New Phytol* 159:539–563.
6. Dutta R, Robinson KR (2004) *Plant Physiol* 135:1398–1406.
7. Feijo JA, Costa SS, Prado AM, Becker JD, Certal AC (2004) *Curr Opin Plant Biol* 7:589–598.
8. Pina C, Pinto F, Feijo JA, Becker JD (2005) *Plant Physiol* 138:744–756.
9. Bock KW, Honys D, Ward JM, Padmanaban S, Nawrocki EP, Hirschi KD, Twell D, Sze H (2006) *Plant Physiol* 140:1151–1168.
10. Moutinho A, Hussey PJ, Trewavas AJ, Malho R (2001) *Proc Natl Acad Sci USA* 98:10481–10486.
11. Kaupp UB, Seifert R (2002) *Physiol Rev* 82:769–824.
12. Talke IN, Blaudez D, Maathuis FJM, Sanders D (2003) *Trends Plant Sci* 8:286–293.
13. Chan CW, Schorrak LM, Smith RK, Jr, Bent AF, Sussman MR (2003) *Plant Physiol* 132:728–731.
14. Li XL, Borsics T, Harrington H, Christopher D (2005) *Funct Plant Biol* 32:643–653.
15. Borsics T, Webb D, Andeme-Ondzighi C, Staehelin LA, Christopher DA (2007) *Planta* 3:563–573.
16. Gobert A, Park G, Amtmann A, Sanders D, Maathuis FJM (2006) *J Exp Bot* 57:791–800.
17. Yoshioka K, Moeder W, Kang HG, Kachroo P, Masmoudi K, Berkowitz G, Klessig DF (2006) *Plant Cell* 18:747–763.
18. Ali R, Ma W, Lemtiri-Chlieh F, Tsaltas D, Leng Q, von Bodman S, Berkowitz GA (2007) *Plant Cell* 19:1081–1095.
19. McElver J, Tzafrir I, Aux G, Rogers R, Ashby C, Smith K, Thomas C, Schetter A, Zhou Q, Cushman MA, *et al.* (2001) *Genetics* 159:1751–1763.
20. Rosso MG, Li Y, Strizhov N, Reiss B, Dekker K, Weisshaar B (2003) *Plant Mol Biol* 53:247–259.
21. Van der Veen JH, Wirtz P (1968) *Euphytica* 17:371–377.
22. Zimmermann P, Hirsch-Hoffmann M, Hennig L, Gruissem W (2004) *Plant Physiol* 136:2621–2632.
23. Schiott M, Romanowsky SM, Baekgaard L, Jakobsen MK, Palmgren MG, Harper JF (2004) *Proc Natl Acad Sci USA* 101:9502–9507.
24. Cho SW, Choi KY, Park CS (2004) *Biochem Biophys Res Commun* 325:525–531.
25. Cho SW, Cho JH, Song HO, Park CS (2005) *Mol Cells* 19:149–154.
26. Biel M, Seeliger M, Pfeifer A, Kohler K, Gerstner A, Ludwig A, Jaissle G, Fauser S, Zrenner E, Hofmann F (1999) *Proc Natl Acad Sci USA* 96:7553–7557.
27. Johnson MA, von Besser K, Zhou Q, Smith E, Aux G, Patton D, Levin JZ, Preuss D (2004) *Genetics* 168:971–982.
28. Procissi A, de Laissardiere S, Ferault M, Vezon D, Pelletier G, Bonhomme S (2001) *Genetics* 158:1773–1783.
29. Becker D, Geiger D, Dunkel M, Roller A, Bertl A, Latz A, Carpaneto A, Dietrich P, Roelfsema MRG, Voelker C, *et al.* (2004) *Proc Natl Acad Sci USA* 101:15621–15626.
30. Mouline K, Very AA, Gaymard F, Boucherez J, Pilot G, Devic M, Bouchez D, Thibaud JB, Sentenac H (2002) *Genes Dev* 16:339–350.
31. Schuurink RC, Shartzer SF, Fath A, Jones RL (1998) *Proc Natl Acad Sci USA* 95:1944–1949.
32. Arazi T, Sunkar R, Kaplan B, Fromm H (1999) *Plant J* 20:171–182.
33. Strunker T, Weyand I, Bonigk W, Van Q, Loogen A, Brown JE, Kashikar N, Hagen V, Krause E, Kaupp UB (2006) *Nat Cell Biol* 8:1149–1154.
34. Galindo BE, de la Vega-Beltran JL, Labarca P, Vacquier VD, Darszon A (2007) *Biochem Biophys Res Commun* 354:668–675.
35. Hua BG, Mercier RW, Zielinski RE, Berkowitz GA (2003) *Plant Physiol Biochem* 41:945–954.
36. Ali R, Zielinski RE, Berkowitz GA (2006) *J Exp Bot* 57:125–138.
37. Ali GS, Reddy VS, Lindgren PB, Jakobek JL, Reddy AS (2003) *Plant Mol Biol* 51:803–815.
38. Moutinho A, Trewavas AJ, Malho R (1998) *Plant Cell* 10:1499–1510.
39. Malho R, Camacho L, Moutinho A (2000) *Ann Bot* 85:59–68.
40. Lord E (2000) *Trends Plants Sci* 5:368–373.
41. Palanivelu R, Preuss D (2000) *Trends Cell Biol* 10:517–524.
42. Coburn CM, Bargmann CI (1996) *Neuron* 17:695–706.
43. Komatsu H, Mori I, Rhee JS, Akaike N, Ohshima Y (1996) *Neuron* 17:707–718.
44. Fischer M, Schnell N, Chattaway J, Davies P, Dixon G, Sanders D (1997) *FEBS Lett* 419:259–262.
45. Clough SJ, Bent AF (1998) *Plant J* 16:735–743.
46. Hellens RP, Edwards EA, Leyland NR, Bean S, Mullineaux PM (2000) *Plant Mol Biol* 42:819–832.
47. Fan LM, Wang YF, Wang H, Wu WH (2001) *J Exp Bot* 52:1603–1614.
48. Lahner B, Gong J, Mahmoudian M, Smith EL, Abid KB, Rogers EE, Guerinot ML, Harper JF, Ward JM, McIntyre L, *et al.* (2003) *Nat Biotechnol* 21:1215–1221.